

Local Search is State of the Art for Neural Architecture Search Benchmarks

Colin White
RealityEngines.AI
colin@realityengines.ai

Sam Nolen
Realityengines.AI
sam@realityengines.ai

Yash Savani
RealityEngines.AI
yash@realityengines.ai

Abstract

Local search is one of the simplest families of algorithms in combinatorial optimization, yet it yields strong approximation guarantees for canonical NP-Complete problems such as the traveling salesman problem and vertex cover. While it is a ubiquitous algorithm in theoretical computer science, local search is often neglected in hyperparameter optimization and neural architecture search.

We show that the simplest local search instantiations achieve state-of-the-art results on multiple NAS benchmarks (NASBench-101 and NASBench-201), outperforming the most popular recent NAS algorithms. However, local search fails to perform well on the much larger DARTS search space. Motivated by these observations, we present a theoretical study which characterizes the performance of local search on graph optimization problems, backed by simulation results. This may be of independent interest beyond NAS. All code and materials needed to reproduce our results are publicly available at https://github.com/realityengines/local_search.

1 Introduction

Neural architecture search (NAS) is a widely popular area of machine learning, with the goal of automating the development of the best neural network for a given dataset. Hundreds of NAS algorithms have been proposed [10, 40], and with the release of two NAS benchmark datasets [8, 39], the extreme computational cost for NAS is no longer a barrier, and it is easier to fairly compare different NAS algorithms. Most of the recently proposed state-of-the-art algorithms are becoming increasingly more complex, many of which use neural networks as subroutines [35, 36]. This trend is problematic because as the complexity of NAS algorithms increases, the amount of necessary “hyper-hyperparameter tuning”, or tuning the NAS algorithm itself, increases. Not only is this a vicious cycle (will we start using AutoML algorithms to tune AutoML algorithms?), but the runtime for any hyper-hyperparameter tuning on a new dataset must be added to the total runtime of the NAS algorithm [19, 38]. Since this information is not always recorded, some NAS algorithms may have under-reported runtimes, making it harder to compare different algorithms.

In contrast to prior work, we study a NAS algorithm which can be implemented in five lines of code (Algorithm 1). Local search is a simple and canonical family of greedy algorithms in combinatorial optimization and has led to famous results in the study of approximation algorithms [6, 11, 23]. The most basic form of local search, often called the hill-climbing algorithm, consists of starting with a random architecture, and then iteratively training all architectures in its neighborhood, choosing the best one for the next iteration. The neighborhood is typically defined as all architectures which differ by one operation or edge. Local search finishes when it reaches a (local or global) optimum, or when it exhausts its runtime budget.

Despite its simplicity, we show that local search achieves state-of-the-art results on all four datasets from the NASBench-101 and NASBench-201 benchmarks, beating out many recent algorithms which claimed state of the art. However, these benchmark datasets contain at most 4×10^5 architectures. On the DARTS [21] search space which contains 10^{18} architectures, we show that local search performs worse than random search. This suggests more generally that strong performance on NAS benchmark datasets does not necessarily imply strong performance on large-scale NAS applications.

Motivated by the stark contrast between the performance of local search on NASBench datasets and DARTS, we present a theoretical study to better understand the performance of local search for NAS on different search spaces. The underlying optimization problem in NAS is a hybrid between discrete optimization, on a graph topology, and continuous optimization, on the distribution of architecture accuracies. We formally define a NAS problem instance by the graph topology, a global probability density function (PDF) on the architecture accuracies, and a local PDF on the accuracies between neighboring architectures, and we derive a set of equations which calculate the probability that a randomly drawn architecture will converge to within ϵ of the global optimum, for all $\epsilon > 0$. As a corollary, we give equations for the expected number of local minima, and the expected size of the preimage of a local minimum. These results completely characterize the performance of local search. To the best of our knowledge, this is the first result which theoretically predicts the performance of a NAS algorithm, and may be of independent interest within discrete optimization. We run simulations which suggest that our theoretical results predict the performance of real datasets reasonably well. Altogether, our results show that the performance of local search depends on the level of *locality* of the search space, as well as the average neighborhood size in the search space. We make available all code and materials needed to reproduce our results.

Our contributions. We summarize our main contributions below.

- We implement the simple local search algorithm as a baseline for NAS, showing that it achieves state-of-the-art performance on two NASBench datasets (which both have size $< 10^6$) as well as subpar performance on a large search space (of size 10^{18}). We suggest that existing NAS benchmarks may be too small to adequately evaluate NAS algorithms.
- We give a full theoretical characterization of the properties of a dataset necessary for local search to give strong performance. We experimentally validate these results on real datasets. Our results improve the theoretical understanding of local search and lay the groundwork for future studies.

2 Related Work

Local search in theoretical computer science. Local search has been studied since at least the 1950s in the context of the traveling salesman problem [5, 7], machine scheduling [26], and graph partitioning [17]. Local search has consistently seen significant attention in theory [1, 3, 15] and practice [4, 14].

Neural architecture search. NAS has gained significant attention in recent years [40], although the first few techniques have been around since at least the 1990s [22, 29]. Popular techniques include Bayesian optimization [16, 13], reinforcement learning [40, 27, 20], gradient descent [21], neural prediction [36, 30], and evolution [28]. NAS can be broadly split into *macro* search, in which the search is over the entire neural network, or *micro* search, in which the search is over a small ‘cell’, which is then duplicated many times to create a large neural network. Recent papers have highlighted the need for fair and reproducible NAS comparisons [18, 19], spurring the release of two cell-based NAS benchmark datasets [8, 39], each of which

include tens of thousands of pretrained neural networks. See the recent survey [10] for a more comprehensive overview on NAS.

Prior work has performed local search for NAS using network morphisms, guided by cosine annealing [9]. This is a more complex variation of local search for NAS. Very recently, concurrent work has also shown that simple local search is a strong baseline for NAS [25]. Their work considers multi-objective NAS (the objective is a function of accuracy and network complexity), focuses on macro search rather than cell-based search, and gives no theoretical results. Therefore, the concurrent work uses different techniques to achieve a similar conclusion. The existence of their work strengthens our conclusions, as they were independently and simultaneously verified.

3 Broader Impact

Our work seeks to improve the understanding of neural architecture search by analyzing the differences between benchmark vs. large-scale search spaces, characterizing the performance of local search, and helping to lay the groundwork for future theoretical results. While this does not have an immediate societal impact the same way that a GAN for deep fakes or a deep learning optimizer for CO₂ emissions would, our work, and more broadly the field of NAS, will be the algorithms powering and refining the deep learning applications with direct societal implications.

Since our work only indirectly affects society, we have less control over its net implications. However, we see two benefits to the AI community that will foster a positive impact. First, we help to lay the groundwork for future theoretical results which can improve our understanding of the workings of different algorithms. Second, we present an easily implementable NAS algorithm which gives strong performance under some settings, and we advocate for simpler NAS algorithms in the future. Not only will this exhibit better baselining of NAS algorithms, but it also helps to democratize neural architecture search. Easily implementable and understandable NAS algorithms will lead to more widespread use. Because of the recent push for explicitly reasoning about the impact of research in AI [12], we are hopeful that downstream deep learning applications will be used to benefit society.

4 Preliminaries

In this section, we formally define the local search algorithm, and we define notation that will be used for the rest of the paper. Given a set A , denote an objective function $\ell : A \rightarrow [0, 1]$. Although our theory works generally for any A and ℓ , we refer to A as a search space of neural architectures, and $\ell(v)$ as the validation loss of $v \in A$ over a fixed dataset and training pipeline. The goal is to find $v^* = \operatorname{argmin}_{v \in A} \ell(v)$, the neural architecture with the minimum validation loss, or else find an architecture whose validation loss is within ϵ of the minimum, for some small $\epsilon > 0$. We define a neighborhood function $N : A \rightarrow 2^A$. For instance, $N(v)$ might represent the set of all neural architectures which differ from v by one operation or edge.

Local search in its simplest form (also called the hill-climbing algorithm) is defined as follows. Start with a random architecture v and evaluate $\ell(v)$ by training v . Iteratively train all architectures in $N(v)$, and then replace v with the architecture u such that $u = \operatorname{argmin}_{w \in N(v)} \ell(w)$. Continue until we reach an architecture v such that $\forall u \in N(v), \ell(v) \leq \ell(u)$, i.e., we reach a local minimum. See Algorithm 1. We often place a runtime bound on the algorithm, in which case the algorithm returns the architecture v with the lowest value of $\ell(v)$ when it exhausts the runtime budget. In Section 6, we also consider two simple variants. In the `query_until_lower` variant, instead of evaluating every architecture in the neighborhood $N(v)$ and picking the best one, we draw architectures $u \in N(v)$ at random without replacement and move to the next iteration

as soon as $\ell(u) < \ell(v)$. In the `continue_at_min` variant, we do not stop at a local minimum, instead moving to the second-best architecture found so far and continuing until we exhaust the runtime budget. One final variant, which we explore in Appendix B, is choosing k initial architectures at random instead of just one, and setting v_1 to be the architecture with the lowest objective value.

Algorithm 1 Local search

Input: Search space A , objective function ℓ , neighborhood function N

1. Pick an architecture $v_1 \in A$ uniformly at random
2. Evaluate $\ell(v_1)$; denote a dummy variable $\ell(v_0) = \infty$; set $i = 1$
3. While $\ell(v_i) < \ell(v_{i-1})$:
 - i. Evaluate $\ell(u)$ for all $u \in N(v_i)$
 - ii. Set $v_{i+1} = \operatorname{argmin}_{u \in N(v_i)} \ell(u)$; set $i = i + 1$

Output: Architecture v_i

Now we define the notation used in Sections 5 and 6. Given a search space A and a neighborhood function N , we define the neighborhood graph $G_N = (A, E_N)$ such that for $u, v \in A$, the edge (u, v) is in E_N if and only if $v \in N(u)$. We only consider symmetric neighborhood functions, that is, $v \in N(u)$ implies $u \in N(v)$. Therefore, we may assume that the neighborhood graph is undirected. Given G, N , and a loss function ℓ , define $\text{LS} : A \rightarrow A$ such that $\forall v \in A$, $\text{LS}(v) = \operatorname{argmin}_{u \in N(v)} \ell(u)$ if $\min_{u \in N(v)} \ell(u) < \ell(v)$, and $\text{LS}(v) = \emptyset$ otherwise. In other words, $\text{LS}(v)$ denotes the architecture after performing one iteration of local search starting from v . For integers $k \geq 1$, recursively define $\text{LS}^k(v) = \text{LS}(\text{LS}^{k-1}(v))$. We set $\text{LS}^0(v) = v$ and denote $\text{LS}^*(v) = \min_{k | \text{LS}^k(v) \neq \emptyset} \text{LS}^k(v)$, that is, the output when running local search to convergence, starting at v . Similarly, define the preimage $\text{LS}^{-k}(v) = \{u \mid \text{LS}^k(u) = v\}$ for integers $k \geq 1$ and $\text{LS}^{-*}(v) = \{u \mid \exists k \geq 0 \text{ s.t. } \text{LS}^{-k}(u) = v\}$. That is, $\text{LS}^{-*}(v)$ is a multifunction which defines the set of all points u which reach v at some point during local search. We refer to LS^{-*} as the full preimage of v .

5 A theory of local search

In this section, we give a theoretical analysis of local search for NAS, including a complete characterization of its performance. We present both a general result on local search, as well as a closed-form solution for search spaces satisfying certain constraints. We give an experimental validation of our theoretical results in the next section.

In a NAS application, the topology of the search space is fixed and discrete, while the distribution of validation losses for architectures is randomized and continuous, due to the non-deterministic nature of training a neural network. For example, both NASBench-101 and NASBench-201 include validation and test accuracies for three different random seeds for each architecture, to better simulate real NAS experiments. Therefore, we assume that the validation loss for a trained architecture is sampled from a global probability distribution, and for each architecture, the validation losses of its neighbors are sampled from a local probability distribution. Given a graph $G_N = (A, E_N)$, each node $v \in A$ has a loss $\ell(v) \in \mathbb{R}$ sampled from a PDF which we denote by pdf_n . For any two neighbors $(v, u) \in E_N$, the PDF for the validation loss x of architecture u is given by $\text{pdf}_e(\ell(v), x)$. Choices for the distribution pdf_e are constrained by the fixed topology of the search space, as well as the distribution pdf_n . In Appendix A, we discuss this further by formally defining measurable spaces for all random variables in our framework.

Our main result is a formula for the fraction of nodes in the search space which are local minima, as

well as a formula for the fraction of nodes v such that the loss of $\text{LS}^*(v)$ is within ϵ of the loss of the global optimum, for all $\epsilon \geq 0$. In other words, we give a formula for the probability that the local search algorithm outputs a solution that is close to optimal. Note that such a formula characterizes the performance of local search. We give the full proofs for all of our results in Appendix A. For the rest of this section, we assume for all $v \in A$, $|N(v)| = s$, and we assume G_N is vertex transitive (given $u, v \in A$, there exists an automorphism of G_N which maps u to v). Let v^* denote the architecture with the global minimum loss, therefore the support of the distribution of validation losses is a subset of $[\ell(v^*), \infty)$. Technically, the integrals in this section are Lebesgue integrals. However, we use the more standard Riemann-Stieltjes notation for clarity. We also slightly abuse notation and define $\text{LS}^{-*}(v) = \text{LS}^{-*}(x)$ when $\ell(v) = x$.

In the following theorems and lemmas, we assume there is a fixed graph G_N , and the validation accuracies are randomly assigned from a distribution defined by pdf_n and pdf_e . Therefore, the expectations are over the random draws from pdf_n and pdf_e .¹

Theorem 5.1. Given $|A| = n$, ℓ , s , ϵ , pdf_n , and pdf_e , we have

$$\begin{aligned} \mathbb{E}[|\{v \in A \mid \text{LS}^*(v) = v\}|] &= n \int_{\ell(v^*)}^{\infty} \text{pdf}_n(x) \left(\int_x^{\infty} \text{pdf}_e(x, y) dy \right)^s dx, \text{ and} \\ \mathbb{E}[|\{v \in A \mid \ell(\text{LS}^*(v)) - \ell(v^*) \leq \epsilon\}|] &= n \int_{\ell(v^*)}^{\ell(v^*) + \epsilon} \text{pdf}_n(x) \left(\int_x^{\infty} \text{pdf}_e(x, y) dy \right)^s \mathbb{E}[|\text{LS}^{-*}(x)|] dx. \end{aligned}$$

Proof sketch. To prove the first statement, we introduce an indicator random variable on the architecture space to test if the architecture is a local minimum: $I(v) = \mathbb{I}\{\text{LS}^*(v) = v\}$. Then

$$\begin{aligned} \mathbb{E}[|\{v \in A \mid \text{LS}^*(v) = v\}|] &= n \cdot \mathcal{P}(\{v \in A \mid I(v) = 1\}) \\ &= n \int_{\ell(v^*)}^{\infty} \text{pdf}_n(x) \cdot \mathcal{P}(\{x < \ell(u) \forall u \text{ s.t. } (u, v) \in E_N, x = \ell(v)\}) dx \\ &= n \int_{\ell(v^*)}^{\infty} \text{pdf}_n(x) \left(\int_x^{\infty} \text{pdf}_e(x, y) dy \right)^s dx. \end{aligned}$$

Intuitively, in the proof of the second statement, we follow similar reasoning but multiply the probability in the outer integral by the expected size of v 's full preimage to weight the integral by the probability a random point will converge to v . Formally, we introduce an indicator random variable on the architecture space that tests if a node will terminate on a local minimum that is within ϵ of the global minimum:

$$\begin{aligned} I_\epsilon(v) &= \mathbb{I}\{\text{LS}^*(v) = u \wedge \ell(u) - \ell(v^*) \leq \epsilon\} \\ &= \mathbb{I}\{\exists S \in \{\text{LS}^{-*}(u) : \text{LS}^*(u) = u \wedge \ell(u) - \ell(v^*) \leq \epsilon\}, v \in S\} \end{aligned}$$

We use this random variable to prove the second statement of the theorem.

¹ In particular, given a node v with validation loss $\ell(v)$ the probability distribution for the validation loss of a neighbor depends only on $\ell(v)$ and pdf_e , which makes the local search procedure similar to a Markov process.

$$\begin{aligned}
\mathbb{E}[\{v \in A \mid \ell(\text{LS}^*(v)) - \ell(v^*) \leq \epsilon\}] &= n \cdot \mathcal{P}(\{I_\epsilon = 1\}) \\
&= n \int_{\ell(v^*)}^{\ell(v^*)+\epsilon} \mathcal{P}(\{v \in A \mid I(v) = 1, \ell(v) = x\}) \mathbb{E}[|\text{LS}^{-*}(x)|] dx \\
&= n \int_{\ell(v^*)}^{\ell(v^*)+\epsilon} \text{pdf}_n(x) \left(\int_{\ell(v)}^{\infty} \text{pdf}_e(x, y) dy \right)^s \mathbb{E}[|\text{LS}^{-*}(x)|] dx
\end{aligned}$$

where the last equality follows from the first half of this theorem. \square

In the next lemma, we derive a recursive equation for $|\text{LS}^{-*}(v)|$. We define the *branching fraction* of graph G_N as $b_k = |N_k(v)| / (|N_{k-1}(v)| \cdot |N(v)|)$, where $N_k(v)$ denotes the set of nodes which are distance k to v in G_N . For example, the branching fraction of a tree with degree d is 1 for all k , and the branching fraction of a clique is $b_1 = 1$ and $b_k = 0$ for all $k > 1$. One more example is as follows. In Appendix B, we show that the neighborhood graph of the NASBench-201 search space is $(K_5)^6$ and therefore its branching factor is $b_k = \frac{6-k+1}{6k}$.

Lemma 5.2. *Given A , ℓ , s , pdf_n , and pdf_e , then for all $v \in A$, we have the following equations.*

$$\mathbb{E}[|\text{LS}^{-1}(v)|] = s \int_{\ell(v)}^{\infty} \text{pdf}_e(\ell(v), y) \left(\int_{\ell(v)}^{\infty} \text{pdf}_e(y, z) dz \right)^{s-1} dy, \text{ and} \quad (5.1)$$

$$\mathbb{E}[|\text{LS}^{-k}(v)|] = b_{k-1} \cdot \mathbb{E}[|\text{LS}^{-1}(v)|] \left(\frac{\int_{\ell(v)}^{\infty} \text{pdf}_e(\ell(v), y) \mathbb{E}[|\text{LS}^{-(k-1)}(y)|] dy}{\int_{\ell(v)}^{\infty} \text{pdf}_e(\ell(v), y) dy} \right). \quad (5.2)$$

For some PDFs, it is not possible to find a closed-form solution for $\mathbb{E}[|\text{LS}^{-k}(v)|]$ because arbitrary functions may not have closed-form antiderivatives. By assuming there exists a function g such that $\text{pdf}_e(x, y) = g(y)$ for all x , we can use induction to find a closed-form expression for $\mathbb{E}[|\text{LS}^{-k}(v)|]$. This includes the uniform distribution ($g(y) = 1$ for $y \in [0, 1]$), as well as distributions that are polynomials in x . In Appendix A, we use this to show that $\mathbb{E}[|\text{LS}^{-*}(v)|]$ can be approximated by $1 + s \cdot G(\ell(v))^s \cdot e^{G(\ell(v))^s}$, where $G(x) = \int_x^{\infty} g(y) dy$. Now we use a similar technique to give a closed-form expression for Theorem 5.1 when the local and global distributions are uniform.

Lemma 5.3. *If $\text{pdf}_n(x) = \text{pdf}_e(x, y) = U([0, 1]) \forall x \in A$, then $\mathbb{E}[\{v \mid v = \text{LS}^*(v)\}] = \frac{n}{s+1}$ and*

$$\mathbb{E}[\{v \mid \ell(\text{LS}^*(v)) - \ell(v^*) \leq \epsilon\}] = n \sum_{i=0}^{\infty} \left(\frac{s^i (1 - (1 - \epsilon)^{(i+1)s+1})}{(i+1)s+1} \cdot \prod_{j=0}^{i-1} \frac{b_j}{js+1} \right).$$

Proof sketch. The probability density function of $U([0, 1])$ is equal to 1 on $[0, 1]$ and 0 otherwise. Then $\int_x^{\infty} \text{pdf}_e(x, y) dy = \int_x^1 dy = (1 - x)$. We use this in combination with Theorem 5.1 to prove the first statement:

$$\mathbb{E}[\{v \mid v = \text{LS}^*(v)\}] = n \int_{\ell(v^*)}^{\infty} 1 \cdot (1 - x)^s dx = \frac{n}{s+1}.$$

To prove the second statement, first we use induction on the recursive expression in Lemma 5.2 to show that for all $v \in A$,

$$\mathbb{E}[|\text{LS}^{-*}(v)|] = \sum_{k=0}^{\infty} \mathbb{E}[|\text{LS}^{-k}(v)|] = \sum_{k=0}^{\infty} \left(s^k (1 - \ell(v))^{sk} \cdot \prod_{i=0}^{k-1} \frac{b_i}{is + 1} \right).$$

We plug this into the second part of Theorem 5.1:

$$\begin{aligned} \mathbb{E}[|\{v \mid \ell(\text{LS}^*(v)) - \ell(v^*) \leq \epsilon\}|] &= n \int_{\ell(v^*)}^{\ell(v^*) + \epsilon} 1 \cdot (1 - x)^s \sum_{k=0}^{\infty} \mathbb{E}[|\text{LS}^{-k}(x)|] dx \\ &= n \int_{\ell(v^*)}^{\ell(v^*) + \epsilon} (1 - x)^s \sum_{k=0}^{\infty} \left(s^k (1 - x)^{sk} \cdot \prod_{i=0}^{k-1} \frac{b_j}{is + 1} \right) dx \\ &= n \sum_{i=0}^{\infty} \left(\frac{s^i (1 - (1 - \epsilon)^{(i+1)s+1})}{(i + 1)s + 1} \cdot \prod_{j=0}^{i-1} \frac{b_j}{js + 1} \right). \end{aligned}$$

□

In the next section, we will show that Theorem 5.1 and Lemma 5.3 can be used to predict the performance of local search.

6 Experiments

In this section, we discuss our experimental setup and results. To promote reproducible research, we discuss how our experiments follow the best practices checklist [19] in Appendix B, and we release our code at https://github.com/realityengines/local_search. In particular, we run experiments on NAS benchmark datasets, we run enough trials to reach statistical significance, and we release our code and all materials needed to reproduce our results. We start by describing the search spaces used in our experiments.

NASBench-101 [39]. The NASBench-101 dataset consists of over 423,000 unique neural architectures from a cell-based search space, and each architecture comes with precomputed validation, and test accuracies for 108 epochs on CIFAR-10. The search space consists of a cell with 7 nodes. The first node is the input, and the last node is the output. The remaining five nodes can be either 1×1 convolution, 3×3 convolution, or 3×3 max pooling. The cell can take on any DAG structure from the input to the output with at most 9 edges.

NASBench-201 [8]. The NASBench-201 dataset consists of $5^6 = 15,625$ unique neural architectures, with precomputed training, validation, and test accuracies for 200 epochs on CIFAR-10, CIFAR-100, and ImageNet-16-120. The search space consists of a cell which is a complete directed acyclic graph over 4 nodes. Therefore, there are $\binom{4}{2} = 6$ edges. Each *edge* takes an operation, and there are five possible operations: 1×1 convolution, 3×3 convolution, 3×3 avg. pooling, skip connect, or none.

DARTS search space [21]. The DARTS search space is a popular search space for large-scale cell-based NAS experiments on CIFAR-10. The search space consists of roughly 10^{18} architectures. It consists of two cells: a convolutional cell and a reduction cell, each with six nodes. The first two nodes are input from previous layers, and the last four nodes can take on any DAG structure such that each node has degree two. Each edge can take one of eight operations.

6.1 Local search performance

We evaluate the effectiveness of local search for NAS. First we compare local search to other NAS algorithms on the four benchmark dataset/search space pairs. On the three NASBench-201 datasets, we compare local search to random search, DNGO [31], Regularized Evolution [28], Bayesian Optimization, BANANAS [36], and NASBOT [16]. On NASBench-101, we test local search with the aforementioned algorithms, as well as REINFORCE [37] and AlphaX [33]. For every algorithm, we used the code directly from the corresponding open source repositories and kept the hyperparameters unchanged for almost all algorithms. For more details on the implementations, see Appendix B. We gave each algorithm a budget of 300 queries. For each algorithm, we recorded the test loss of the architecture with the best validation loss that has been queried so far. We ran 200 trials of each algorithm and averaged the results. For local search, we set $N(v)$ to denote all architectures which differ by one operation or edge. If local search converged before its budget, it started a new run. On NASBench-101 and ImageNet-16-120, we used the query_until_lower variant of local search, and on NASBench-201 CIFAR-10 and CIFAR-100, we used the continue_at_min variant. (In Appendix B, we evaluate all four variants.) See Figure 6.3. Local search consistently performs the strongest on all four datasets. Random search performed significantly worse than all other algorithms on NASBench-201, so we omitted it from the plots. Note that on ImageNet16-120, some algorithms such as NASBOT overfit to the training set, causing performance to decline over time.

In Appendix B, we evaluate local search with a different number k of random initializations, showing that there is little effect on the performance when $k \leq 20$. We also report local search statistics such as the number of local minima and the average number of iterations to convergence.

Next, we evaluate local search with the query_until_lower variant on the DARTS search space. We ran one trial training all queried architecture to 25 epochs, and another trial training to 50 epochs. The runtime is 11.8 GPU days on a Tesla V100. We trained the final returned architectures for 600 epochs, using the same training pipeline as prior work [18, 21]. See Table 1. Local search performed worse than random search, and significantly worse than DARTS. One reason for the subpar performance is because the degree of the neighborhood graph is 136, much larger than NASBench-201’s 24. For instance, in the 50 epoch trial, 100 queries and 11.8 GPU days was not sufficient to get through a single iteration of local search even with the query_until_lower variant.

Discussion. The simple local search algorithm achieved state-of-the-art performance on all four NAS benchmark search space/datasets, beating out several popular NAS algorithms. However, the poor performance on DARTS shows that local search is not efficient on search spaces with high degree. As a consequence, we suggest that existing NAS benchmarks including NASBench-101 and -201 may be too small and/or simple to adequately evaluate NAS algorithms. For example, while NASBench-201 contains 15k architectures, the DARTS search space contains 10^{18} architectures, and similarly the search spaces from ENAS [27] and PNAS [20] contain 10^{11} and 10^{14} architectures. Since local search can be implemented in five lines of code, we encourage local search to be used as a benchmark in future work, especially when experimenting on smaller search spaces.

Table 1: Percent error on the test set of the best architectures returned by several NAS algorithms. The runtime is in total GPU-days on a Tesla V100.

NAS Algorithm	Source	Test error	Queries	Runtime
Random search	[21]	3.29		4
DARTS	[21]	2.68		5
ASHA	[18]	3.08	700	9
BANANAS	[36]	2.64	100	11.8
Local Search 50 epochs	Ours	3.49	100	11.8
Local Search 25 epochs	Ours	3.93	200	11.8

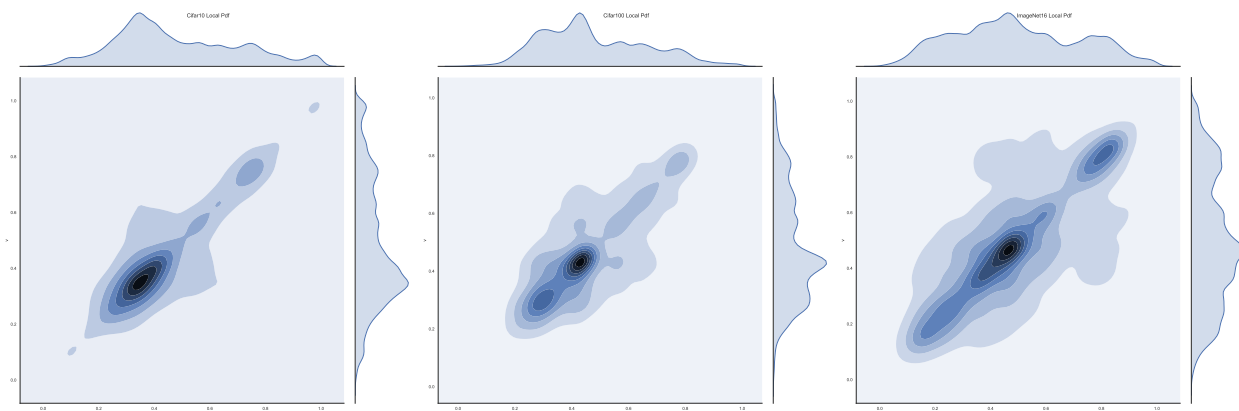


Figure 6.1: Probability density function for CIFAR-10 (left), CIFAR-100 (middle), and ImageNet16-120 (right) on NASBench-201. For each coordinate (u, v) , a darker color indicates that architectures with accuracy u and v are more likely to be neighbors.

Simulation Results. We run a local search simulation using the equations in Section 5 as a means of experimentally validating our theoretical results with real data (we use NASBench-201). In order to use these equations, first we must approximate the local and global probability density functions of the three datasets in NASBench-201. We start by visualizing the probability density functions of the three datasets See Figure 6.1. We see the most density along the diagonal, meaning that architectures with similar accuracy are more likely to be neighbors. Therefore, we can approximate the PDFs by using the following equation:

$$\text{pdf}(u) = \begin{cases} \frac{1}{\sigma\sqrt{2\pi}} \cdot e^{-\frac{1}{2}\left(\frac{u-v}{\sigma}\right)^2} \cdot \left(\int_0^1 \frac{1}{\sigma\sqrt{2\pi}} \cdot e^{-\frac{1}{2}\left(\frac{w-v}{\sigma}\right)^2} dw\right)^{-1} & \text{if } u \in [0, 1], \\ 0 & \text{otherwise.} \end{cases} \quad (6.1)$$

This is a normal distribution with mean $u - v$ and standard deviation of σ , truncated so that it is a valid PDF in $[0, 1]$. To model the global PDF for each dataset, we plot a histogram of the validation losses and match them to the closest-fitting values of σ and v . See Figure 6.2. The best values of σ are 0.18, 0.1, and 0.22 for CIFAR-10, CIFAR-100, and ImageNet16-120, respectively, and the best values for v are all 0.25.² To model the local PDF for each dataset, we compute the random walk autocorrelation (RWA) on each dataset. RWA is

² Note that plotting a histogram of all validation losses is impractical for real-world NAS search spaces; we do this on NASBench-201 as a means of validating our theoretical results.

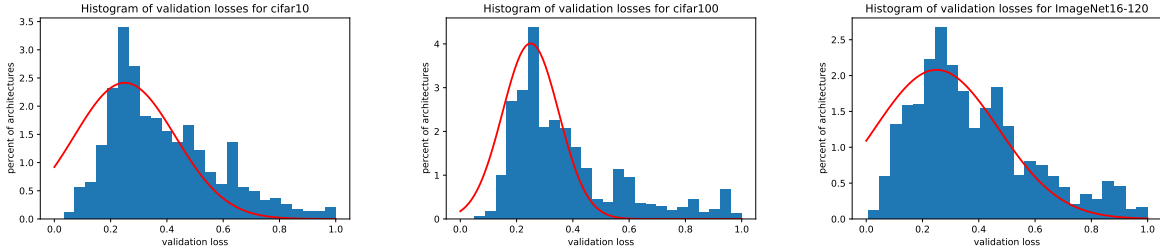


Figure 6.2: Histogram of validation losses for the three datasets in NASBench-201, fitted with the best values of σ and v in Equation 6.1.

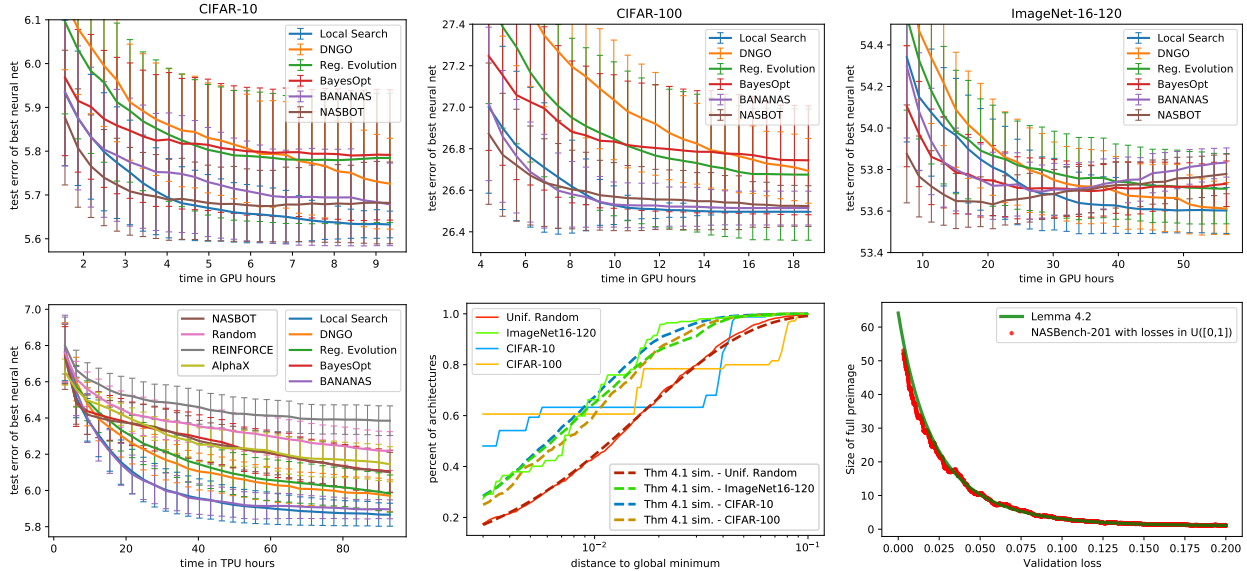


Figure 6.3: Results for NAS algorithms on NASBench-201 (top) and NASBench-101 (bottom left). Probability that local search will converge to within ϵ of the global optimum, compared to Theorem 5.1 (bottom middle). Validation loss vs. size of preimages, compared to Lemma 5.2 (bottom right).

defined as the autocorrelation of the accuracies of points visited during a random walk on the neighborhood graph [34, 32], and was used to measure locality in NASBench-101 in prior work [39]. For the full details of how we modeled the datasets in NASBench-201, see Appendix B.

Now we use Theorem 5.1 to compute the probability that a randomly drawn architecture will converge to within ϵ of the global minimum when running local search. Since there is no closed-form solution for the expression in Lemma 5.2, we compute Theorem 5.1 up to the 5th preimage. We compare this to the experimental results on NASBench-201. We also compare the performance of the NASBench-201 search space with validation losses drawn uniformly at random, to the performance predicted by Lemma 5.3. Finally, we compare the preimage sizes of the architectures in NASBench-201 with randomly drawn validation losses to the sizes predicted in Lemma 5.2. See Figure 6.3. Our theory exactly predicts the performance and the preimage sizes of the uniform random NASBench-201 dataset. On the three image datasets, our theory predicts the performance fairly accurately, but is not perfect due to our assumption that the distribution of accuracies is unimodal.

7 Conclusion

We show that the simplest local search algorithm achieves state-of-the-art results on the most popular existing NAS benchmarks (NASBench-101 and NASBench-201). We also show that it has subpar performance on the DARTS search space, suggesting that the NAS benchmarks may be too simple and/or small to adequately evaluate NAS methods. Since local search is a simple technique that sometimes gives state-of-the-art performance, we encourage local search to be used as a benchmark for NAS in the future, especially for smaller search spaces.

Motivated by the stark contrast between the performance of local search on NASBench datasets and DARTS, we give a theoretical study which explains the performance of local search for NAS on different search spaces. We define a probabilistic graph optimization framework to study NAS problems, and we give a characterization of the performance of local search for NAS in our framework. In particular, we find that local search performs well on search spaces with high locality and with a neighborhood graph of low degree. Our theoretical results may be of independent interest. We validate our theory with experimental results. Investigating more sophisticated variants of local search for NAS such as Tabu search, simulated annealing, or multi-fidelity local search, are interesting next steps.

Acknowledgements

We thank Willie Neiswanger and Murali Narayanaswamy for their help with this project.

References

- [1] E Aarts and JK Lenstra. Local search in combinatorial optimization. *John Wiley & Sons, Inc.*, 1997.
- [2] Milton Abramowitz and Irene A Stegun. *Handbook of mathematical functions with formulas, graphs, and mathematical tables*, volume 55. 1948.
- [3] Maria-Florina Balcan, Nika Haghtalab, and Colin White. K-center clustering under perturbation resilience. *ACM Trans. Algorithms*, 16(2), 2020.
- [4] Jon Jouis Bentley. Fast algorithms for geometric traveling salesman problems. *ORSA Journal on computing*, 4(4):387–411, 1992.
- [5] Frederick Bock. An algorithm for solving travelling-salesman and related network optimization problems. In *Operations Research*, volume 6, pages 897–897, 1958.
- [6] Vincent Cohen-Addad, Philip N Klein, and Claire Mathieu. Local search yields approximation schemes for k-means and k-median in euclidean and minor-free metrics. In *Proceedings of the Annual Symposium on Foundations of Computer Science (FOCS)*, pages 353–364, 2016.
- [7] Georges A Croes. A method for solving traveling-salesman problems. *Operations research*, 6(6):791–812, 1958.
- [8] Xuanyi Dong and Yi Yang. Nas-bench-201: Extending the scope of reproducible neural architecture search. In *Proceedings of the International Conference on Learning Representations (ICLR)*, 2020.
- [9] Thomas Elsken, Jan-Hendrik Metzen, and Frank Hutter. Simple and efficient architecture search for convolutional neural networks. *arXiv preprint arXiv:1711.04528*, 2017.
- [10] Thomas Elsken, Jan Hendrik Metzen, and Frank Hutter. Neural architecture search: A survey. *arXiv preprint arXiv:1808.05377*, 2018.
- [11] Zachary Friggstad, Mohsen Rezapour, and Mohammad R Salavatipour. Local search yields a ptas for k-means in doubling metrics. *SIAM Journal on Computing*, 48(2):452–480, 2019.
- [12] Brent Hecht, Lauren Wilcox, Jeffrey P Bigham, Johannes Schöning, Ehsan Hoque, Jason Ernst, Yonatan Bisk, Luigi De Russis, Lana Yarosh, Bushra Anjum, Danish Contractor, and Cathy Wu. It’s time to do something: Mitigating the negative impacts of computing through a change to the peer review process. *ACM Future of Computing Blog*, 2018.
- [13] Haifeng Jin, Qingquan Song, and Xia Hu. Auto-keras: Efficient neural architecture search with network morphism. *arXiv preprint arXiv:1806.10282*, 2018.
- [14] David S Johnson and Lyle A McGeoch. The traveling salesman problem: A case study in local optimization. *Local search in combinatorial optimization*, 1(1):215–310, 1997.
- [15] David S Johnson, Christos H Papadimitriou, and Mihalis Yannakakis. How easy is local search? *Journal of computer and system sciences*, 37(1):79–100, 1988.
- [16] Kirthevasan Kandasamy, Willie Neiswanger, Jeff Schneider, Barnabas Poczos, and Eric P Xing. Neural architecture search with bayesian optimisation and optimal transport. In *Advances in Neural Information Processing Systems*, pages 2016–2025, 2018.

- [17] Brian W Kernighan and Shen Lin. An efficient heuristic procedure for partitioning graphs. *The Bell system technical journal*, 49(2):291–307, 1970.
- [18] Liam Li and Ameet Talwalkar. Random search and reproducibility for neural architecture search. *arXiv preprint arXiv:1902.07638*, 2019.
- [19] Marius Lindauer and Frank Hutter. Best practices for scientific research on neural architecture search. *arXiv preprint arXiv:1909.02453*, 2019.
- [20] Chenxi Liu, Barret Zoph, Maxim Neumann, Jonathon Shlens, Wei Hua, Li-Jia Li, Li Fei-Fei, Alan Yuille, Jonathan Huang, and Kevin Murphy. Progressive neural architecture search. In *Proceedings of the European Conference on Computer Vision (ECCV)*, pages 19–34, 2018.
- [21] Hanxiao Liu, Karen Simonyan, and Yiming Yang. Darts: Differentiable architecture search. *arXiv preprint arXiv:1806.09055*, 2018.
- [22] Krzysztof Maziarz, Andrey Khorlin, Quentin de Laroussilhe, and Andrea Gesmundo. Evolutionary-neural hybrid agents for architecture search. *arXiv preprint arXiv:1811.09828*, 2018.
- [23] Wil Michiels, Emile Aarts, and Jan Korst. *Theoretical aspects of local search*. Springer Science & Business Media, 2007.
- [24] Willie Neiswanger, Kirthevasan Kandasamy, Barnabas Poczos, Jeff Schneider, and Eric Xing. Probo: a framework for using probabilistic programming in bayesian optimization. *arXiv preprint arXiv:1901.11515*, 2019.
- [25] T Den Ottelander, A Dushatskiy, M Virgolin, and Peter AN Bosman. Local search is a remarkably strong baseline for neural architecture search. *arXiv preprint arXiv:2004.08996*, 2020.
- [26] ES Page. An approach to the scheduling of jobs on machines. *Journal of the Royal Statistical Society: Series B (Methodological)*, 23(2):484–492, 1961.
- [27] Hieu Pham, Melody Y Guan, Barret Zoph, Quoc V Le, and Jeff Dean. Efficient neural architecture search via parameter sharing. *arXiv preprint arXiv:1802.03268*, 2018.
- [28] Esteban Real, Alok Aggarwal, Yanping Huang, and Quoc V Le. Regularized evolution for image classifier architecture search. In *Proceedings of the AAAI conference on artificial intelligence*, volume 33, pages 4780–4789, 2019.
- [29] Syed Asif Raza Shah, Wenji Wu, Qiming Lu, Liang Zhang, Sajith Sasidharan, Phil DeMar, Chin Guok, John Macauley, Eric Pouyoul, Jin Kim, et al. Amoebanet: An sdn-enabled network service for big data science. *Journal of Network and Computer Applications*, 119:70–82, 2018.
- [30] Han Shi, Renjie Pi, Hang Xu, Zhenguo Li, James T Kwok, and Tong Zhang. Multi-objective neural architecture search via predictive network performance optimization. *arXiv preprint arXiv:1911.09336*, 2019.
- [31] Jasper Snoek, Oren Rippel, Kevin Swersky, Ryan Kiros, Nadathur Satish, Narayanan Sundaram, Mostofa Patwary, Mr Prabhat, and Ryan Adams. Scalable bayesian optimization using deep neural networks. In *International conference on machine learning*, pages 2171–2180, 2015.

- [32] Peter F Stadler. Landscapes and their correlation functions. *Journal of Mathematical chemistry*, 20(1), 1996.
- [33] Linnan Wang, Yiyang Zhao, Yuu Jinnai, and Rodrigo Fonseca. Alphax: exploring neural architectures with deep neural networks and monte carlo tree search. *arXiv preprint arXiv:1805.07440*, 2018.
- [34] Edward Weinberger. Correlated and uncorrelated fitness landscapes and how to tell the difference. *Biological cybernetics*, 63(5), 1990.
- [35] Wei Wen, Hanxiao Liu, Hai Li, Yiran Chen, Gabriel Bender, and Pieter-Jan Kindermans. Neural predictor for neural architecture search. *arXiv preprint arXiv:1912.00848*, 2019.
- [36] Colin White, Willie Neiswanger, and Yash Savani. Bananas: Bayesian optimization with neural architectures for neural architecture search. *arXiv preprint arXiv:1910.11858*, 2019.
- [37] Ronald J Williams. Simple statistical gradient-following algorithms for connectionist reinforcement learning. *Machine learning*, pages 229–256, 1992.
- [38] Antoine Yang, Pedro M Esperança, and Fabio M Carlucci. Nas evaluation is frustratingly hard. In *Proceedings of the International Conference on Learning Representations (ICLR)*, 2020.
- [39] Chris Ying, Aaron Klein, Esteban Real, Eric Christiansen, Kevin Murphy, and Frank Hutter. Nas-bench-101: Towards reproducible neural architecture search. *arXiv preprint arXiv:1902.09635*, 2019.
- [40] Barret Zoph and Quoc V. Le. Neural architecture search with reinforcement learning. In *Proceedings of the International Conference on Learning Representations (ICLR)*, 2017.

A Details from Section 5

In this section, we give details from Section 5. For convenience, we restate all theorems and lemmas here.

We start by formally defining all measurable spaces in our theoretical framework. Recall that the topology of the search space is fixed and discrete, while the distribution of validation losses for architectures is randomized and continuous. This is because training a neural network is not deterministic; in fact, both NASBench-101 and NASBench-201 include validation and test accuracies for three different random seeds for each architecture, to better simulate real NAS experiments. Therefore, we assume that the validation loss for a trained architecture is sampled from a global probability distribution, and for each architecture, the validation losses of its neighbors are sampled from a local probability distribution.

Let $(\mathbb{R}, \mathcal{B}(\mathbb{R}))$ denote a measurable space for the global validation losses induced by the dataset on the architectures, where $\mathcal{B}(\mathbb{R})$ is the Borel σ -algebra on \mathbb{R} . The distribution for the validation loss of any architecture in the search space is given by $\text{pdf}_n(x) \forall x \in \mathbb{R}$.

Let $(\mathbb{R}^2, \mathcal{B}(\mathbb{R}^2))$ denote a measurable space for validation losses in a neighborhood of an architecture. Let $E : \mathbb{R}^2 \rightarrow \mathbb{R}$ denote a random variable mapping the validation losses of two neighboring architectures to the loss of the second architecture, $E(x, y) \mapsto y$. E has a distribution that is characterized by probability density function $\text{pdf}_e(x, y) \forall x, y \in \mathbb{R}$. This gives us a probability over the validation loss for a neighboring architecture.

Every architecture $v \in A$ has a loss $\ell(v) \in \mathbb{R}$ that is sampled from pdf_n . For any two neighbors $(v, u) \in E_N$, the PDF for the validation loss x of architecture u is given by $\text{pdf}_e(\ell(v), x)$. Note that choices for the distribution pdf_e are constrained by the fixed topology of the search space, as well as the selected distribution pdf_n . Let $(A, 2^A)$ denote a measurable space over the nodes of the graph.

For the rest of this section, we fix an arbitrary neighborhood graph G_N with vertex set A such that for all $v \in A$, $|N(v)| = s$, i.e., G_N has regular degree s , and we assume that G_N is vertex transitive. Each vertex in A is assigned a validation loss according to pdf_n and pdf_e defined above. The expectations in the following theorem and lemmas are over the random draws from pdf_n and pdf_e .

Theorem 5.1. Given $|A| = n$, ℓ , s , ϵ , pdf_n , and pdf_e , we have

$$\begin{aligned} \mathbb{E}[|\{v \in A \mid \text{LS}^*(v) = v\}|] &= n \int_{\ell(v^*)}^{\infty} \text{pdf}_n(x) \left(\int_x^{\infty} \text{pdf}_e(x, y) dy \right)^s dx, \text{ and} \\ \mathbb{E}[|\{v \in A \mid \ell(\text{LS}^*(v)) - \ell(v^*) \leq \epsilon\}|] &= n \int_{\ell(v^*)}^{\ell(v^*) + \epsilon} \text{pdf}_n(x) \left(\int_x^{\infty} \text{pdf}_e(x, y) dy \right)^s \mathbb{E}[|\text{LS}^{-*}(x)|] dx. \end{aligned}$$

Proof. To prove the first statement, we introduce an indicator random variable on the architecture space to test if the architecture is a local minimum $I : A \rightarrow \mathbb{R}$, where

$$\begin{aligned} I(v) &= \mathbb{I}\{\text{LS}^*(v) = v\} \\ &= \mathbb{I}\{\ell(v) < \ell(u) \forall u \text{ s.t. } (u, v) \in E_N\}. \end{aligned}$$

The expected number of local minima in $|A|$ is equal to $|A|$ times the fraction of nodes in A which are local minima. Therefore, we have

$$\begin{aligned}
\mathbb{E}[|\{v \in A \mid \text{LS}^*(v) = v\}|] &= n \cdot \mathcal{P}(\{I = 1\}) \\
&= n \int_{-\infty}^{\infty} \text{pdf}_n(x) \cdot \mathcal{P}(\{x < \ell(u) \forall u \text{ s.t. } (u, v) \in E_N, x = \ell(v)\}) dx \\
&= n \int_{-\infty}^{\infty} \text{pdf}_n(x) \left(\int_x^{\infty} \text{pdf}_e(x, y) dy \right)^s dx
\end{aligned}$$

In line one we use the notation $\mathcal{P}(\{I = 1\}) \equiv \mathcal{P}(\{v \in A \mid I(v) = 1\})$.

To prove the second statement, we introduce an indicator random variable on the architecture space that tests if a node will terminate on a local minimum that is within ϵ of the global minimum, $I_\epsilon : A \rightarrow \mathbb{R}$, where

$$\begin{aligned}
I_\epsilon(v) &= \mathbb{I}\{\text{LS}^*(v) = u \wedge l(u) - l(v^*) \leq \epsilon\} \\
&= \mathbb{I}\{\exists S \in \{\text{LS}^{-*}(u) : \text{LS}^*(u) = u \wedge l(u) - l(v^*) \leq \epsilon\}, v \in S\}
\end{aligned}$$

We use this random variable to prove the second statement of the theorem.

$$\begin{aligned}
\mathbb{E}[|\{v \in A \mid \ell(\text{LS}^*(v)) - \ell(v^*) \leq \epsilon\}|] &= n \cdot \mathcal{P}(\{I_\epsilon = 1\}) \\
&= n \int_{\ell(v^*)}^{\ell(v^*) + \epsilon} \mathcal{P}(\{v \in A \mid I(v) = 1, \ell(v) = x\}) \mathbb{E}[|\text{LS}^{-*}(x)|] dx \\
&= n \int_{\ell(v^*)}^{\ell(v^*) + \epsilon} \text{pdf}_n(x) \left(\int_{\ell(v)}^{\infty} \text{pdf}_e(x, y) dy \right)^s \mathbb{E}[|\text{LS}^{-*}(x)|] dx
\end{aligned}$$

where the last equality follows from the first half of this theorem. This concludes the proof. \square

Recall that we defined the *branching fraction* of graph G_N as $b_k = |N_k(v)| / (|N_{k-1}(v)| \cdot |N(v)|)$, where $N_k(v)$ denotes the set of nodes which are distance k to v in G_N . For example, the branching fraction of a tree with degree d is 1 for all k , and the branching fraction of a clique is $b_1 = 1$ and $b_k = 0$ for all $k > 1$. Also, for any graph, $b_1 = 1$. We will see in Section B that the neighborhood graph of the NASBench-201 search space is $(K_5)^6$ and therefore its branching factor is $b_k = \frac{6-k+1}{6k}$.

Now we restate and prove Lemma 5.2, which gives a formula for the k 'th preimage of the local search function.

Lemma 5.2. *Given A , ℓ , s , pdf_n , and pdf_e , then for all $v \in A$, we have the following equations.*

$$\mathbb{E}[|\text{LS}^{-1}(v)|] = s \int_{\ell(v)}^{\infty} \text{pdf}_e(\ell(v), y) \left(\int_{\ell(v)}^{\infty} \text{pdf}_e(y, z) dz \right)^{s-1} dy, \text{ and} \quad (5.1)$$

$$\mathbb{E}[|\text{LS}^{-k}(v)|] = b_{k-1} \cdot \mathbb{E}[|\text{LS}^{-1}(v)|] \left(\frac{\int_{\ell(v)}^{\infty} \text{pdf}_e(\ell(v), y) \mathbb{E}[|\text{LS}^{-(k-1)}(y)|] dy}{\int_{\ell(v)}^{\infty} \text{pdf}_e(\ell(v), y) dy} \right). \quad (5.2)$$

Proof. The function $\text{LS}^{-1}(v) \in 2^A$ returns a set of nodes which form the preimage of node $v \in A$, namely, the set of all neighbors $u \in N(v)$ with higher validation loss than v , and whose neighbors $w \in N(u)$ excluding v have higher validation loss than $\ell(v)$. Formally,

$$\begin{aligned} \text{LS}^{-1}(v) &= \{u \in A \mid \text{LS}(u) = v\} \\ &= \{u \in A \mid (v, u) \in E_N, \ell(v) < \ell(u), \{v' \in A \setminus \{v\} \mid (v', u) \in E_N, \ell(v') < \ell(v)\} = \emptyset\}. \end{aligned}$$

Let $\text{LS}_v^{-1} : A \rightarrow \mathbb{R}$ denote a random variable where $\text{LS}_v^{-1}(u) = \mathbb{I}\{u \in \text{LS}^{-1}(v)\}$. The probability distribution for LS_v^{-1} gives the probability that a neighbor of v is in the preimage of v . We can multiply this probability by $|N(v)| = s$ to express the expected number of nodes in the preimage of v .

$$\begin{aligned} \mathbb{E}[|\text{LS}^{-1}(v)|] &= s \cdot \mathcal{P}(\{\text{LS}_v^{-1} = 1\}) \\ &= s \int_{\ell(v)}^{\infty} \text{pdf}_e(\ell(v), y) \left(\int_{\ell(v)}^{\infty} \text{pdf}_e(y, z) dz \right)^{s-1} dy. \end{aligned}$$

Note that the inner integral is raised to the power of $s - 1$, not s , so as not to double count node v . We can use this result to find the preimage of node v after m steps. Let $\text{LS}_v^{-m} : A \rightarrow \mathbb{R}$ denote a random variable where

$$\begin{aligned} \text{LS}_v^{-m}(u) &= \mathbb{I}\{u \in \text{LS}^{-m}(v)\} \\ &= \mathbb{I}\{\forall w \in \text{LS}^{-1}(v), u \in \text{LS}^{-(m-1)}(w)\}. \end{aligned}$$

Following a similar argument as above, we compute the expected size of the m 'th preimage set.

$$\begin{aligned} \mathbb{E}[|\text{LS}^{-m}(v)|] &= b_{k-1} \cdot \mathbb{E}[|\text{LS}^{-1}(v)|] \cdot \mathbb{E}[\{\forall w \in A \mid \forall u \in \text{LS}^{-1}(v), \text{LS}_u^{-(m-1)}(w) = 1\}] \\ \mathbb{E}[|\text{LS}^{-m}(v)|] &= b_{k-1} \cdot \mathbb{E}[|\text{LS}^{-1}(v)|] \left(\frac{\int_{\ell(v)}^{\infty} \text{pdf}_e(\ell(v), y) \mathbb{E}[|\text{LS}^{-(m-1)}(y)|] dy}{\int_{\ell(v)}^{\infty} \text{pdf}_e(\ell(v), y) dy} \right) \end{aligned}$$

□

Closed-form solution for single-variate PDFs. Now we give the details for Lemma 5.3. We start with a lemma that will help us prove Lemma 5.3. This lemma uses induction to derive a closed-form solution to Lemma 5.2 in the case where $\text{pdf}_e(x, y)$ is independent of x .

Lemma A.1. Assume there exists a function g such that $\text{pdf}_e(x, y) = g(y)$ for all x . Given $v \in A$, for $k \geq 1$,

$$\mathbb{E}[|\text{LS}^{-k}(v)|] = s^k \left(\int_{\ell(v)}^{\infty} g(y) dy \right)^{sk} \cdot \prod_{i=0}^{k-1} \frac{b_i}{is + 1}.$$

Proof. Given $v \in A$,

$$\begin{aligned}
\mathbb{E}[|\text{LS}^{-1}(v)|] &= s \int_{\ell(v)}^{\infty} \text{pdf}_e(\ell(v), y) \left(\int_{\ell(v)}^{\infty} \text{pdf}_e(y, z) dz \right)^{s-1} dy \\
&= s \int_{\ell(v)}^{\infty} g(y) \left(\int_{\ell(v)}^{\infty} g(z) dz \right)^{s-1} dy \\
&= s \left(\int_{\ell(v)}^{\infty} g(y) dy \right)^s,
\end{aligned}$$

where the first equality follows from Lemma 5.2. Now we give a proof by induction for the closed-form equation. The base case, $m = 1$, is proven above. Given an integer $m \geq 1$, assume that

$$\mathbb{E}[|\text{LS}^{-m}(v)|] = s^m \left(\int_{\ell(v)}^{\infty} g(y) dy \right)^{sn} \cdot \prod_{i=0}^{m-1} \frac{b_i}{is + 1}.$$

Then

$$\begin{aligned}
\mathbb{E}[|\text{LS}^{-(m+1)}(v)|] &= b_n \cdot \mathbb{E}[|\text{LS}^{-1}(v)|] \cdot \left(\int_{\ell(v)}^{\infty} g(y) dy \right)^{-1} \int_{\ell(v)}^{\infty} g(y) \mathbb{E}[|\text{LS}^{-m}(y)|] dy \\
&= b_n \cdot s \left(\int_{\ell(v)}^{\infty} g(y) dy \right)^s \left(\int_{\ell(v)}^{\infty} g(y) dy \right)^{-1} \int_{\ell(v)}^{\infty} g(y) \cdot \mathbb{E}[|\text{LS}^{-m}(y)|] dy \\
&= b_n \cdot s \left(\int_{\ell(v)}^{\infty} g(y) dy \right)^{s-1} \int_{\ell(v)}^{\infty} g(y) \cdot s^m \left(\int_y^{\infty} g(z) dz \right)^{sn} \cdot \prod_{i=0}^{m-1} \frac{b_i}{is + 1} \cdot dy \\
&= b_n \cdot s^{m+1} \left(\int_{\ell(v)}^{\infty} g(y) dy \right)^{s-1} \cdot \prod_{i=0}^{m-1} \frac{b_i}{is + 1} \int_{\ell(v)}^{\infty} g(y) \left(\int_y^{\infty} g(z) dz \right)^{sn} dy \\
&= b_n \cdot s^{m+1} \left(\int_{\ell(v)}^{\infty} g(y) dy \right)^{s-1} \cdot \prod_{i=0}^{m-1} \frac{b_i}{is + 1} \left(\int_{\ell(v)}^{\infty} g(z) dz \right)^{sn+1} \frac{1}{sn + 1} \\
&= s^{m+1} \left(\int_{\ell(v)}^{\infty} g(y) dy \right)^{s(m+1)} \cdot \prod_{i=0}^m \frac{b_i}{is + 1}.
\end{aligned}$$

In the first equality, we used Lemma 5.2, and in the fourth equality, we used the fact that

$$\frac{\partial}{\partial y} \left(\int_y^{\infty} g(z) dz \right)^{sm+1} = g(y) \left(\int_y^{\infty} g(z) dz \right)^{sm} (sm + 1).$$

This concludes the proof. \square

Next, we prove a lemma which gives strong approximation guarantees on the size of the full preimage of an architecture, again assuming that $\text{pdf}_e(x, y)$ is independent if x . For this lemma, we need to assume that n is large compared to s . However, this is the only lemma that assumes n is large. In particular, Lemma 5.3 will not need this assumption.

Lemma A.2. Assume there exists g such that $\text{pdf}_e(x, y) = g(y)$ for all x . Denote $G(x) = \int_x^\infty g(y)dy$. Given s , there exists N such that for all $n > N$, for all v , we have

$$1 + s \cdot G(\ell(v))^s e^{\frac{s}{s+1}G(\ell(v))^s} \leq \mathbb{E}[|LS^{*-}(v)|] \leq 1 + s \cdot G(\ell(v))^s \cdot e^{G(\ell(v))^s}.$$

Proof. From Lemma A.1, we have

$$\mathbb{E}[|LS^{*-}(v)|] = \sum_{m=1}^{\infty} \mathbb{E}[|LS^{-m}(v)|] = \sum_{m=1}^{\infty} \left(s^m G(\ell(v))^{sm} \cdot \prod_{i=0}^{m-1} \frac{b_i}{is+1} \right). \quad (\text{A.1})$$

We start with the upper bound. For all $j \geq 1$, $\frac{s \cdot b_j}{js+1} \leq \frac{s}{js+1} \leq \frac{s}{sj} = \frac{1}{j}$ because $0 \leq b_j \leq 1$ for all $1 \leq j$. Therefore for all i ,

$$\prod_{j=1}^{i-1} \frac{s \cdot b_j}{js+1} \leq \prod_{j=1}^{i-1} \frac{1}{j} = \frac{1}{(i-1)!}.$$

It follows that

$$\begin{aligned} \mathbb{E}[|LS^{-m}(v)|] &= \sum_{i=1}^{\infty} s^i G(\ell(v))^{si} \prod_{j=0}^{i-1} \frac{b_j}{js+1} \\ &= s \sum_{i=1}^{\infty} G(\ell(v))^s \prod_{j=1}^{i-1} \frac{s \cdot b_j}{js+1} \\ &\leq s G(\ell(v))^s \sum_{i=1}^{\infty} \left(\frac{1}{(i-1)!} \cdot G(\ell(v))^s \right) \\ &= s G(\ell(v))^s e^{G(\ell(v))^s}. \end{aligned}$$

The final equality comes from the well-known Taylor series $e^x = \sum_{n=0}^{\infty} \frac{x^n}{n!}$ (e.g. [2]) evaluated at $x = G(\ell(v))^s$.

Now we prove the lower bound. $b_1 = 1$ by definition for all graphs, and for $1 < j \leq D$, $0 \leq b_j \leq 1$, where D denotes the diameter of the graph. (Since $N_D(v) = n$ for all v , b_j is meaningless for $j \geq D$.) Recall that all of our arguments assume vertex transitivity. It follows that $b_{D-1} \leq b_{D-2} \leq \dots \leq b_1$. Now, for a fixed s , b_{D-1} approaches 1 as n approaches infinity. Therefore, given s , there exists N such that for all $n > N$, $b_{D-1} > \frac{2s+1}{2(s+1)}$. Then for all i ,

$$\frac{1}{j(s+1)} \leq \frac{1}{js+1} \left(\frac{js+1}{j(s+1)} \right) \leq \frac{1}{js+1} \left(\frac{2s+1}{2(s+1)} \right) \leq \frac{1}{js+1} (b_{D-1}) \leq \frac{b_j}{js+1}.$$

Therefore,

$$\frac{s^{i-1}}{(i-1)!(s+1)^{i-1}} = \prod_{j=1}^{i-1} \frac{s}{j(s+1)} \leq \prod_{j=1}^{i-1} \frac{s \cdot b_j}{js+1}.$$

It follows that

$$\begin{aligned}
\mathbb{E}[|\text{LS}^{-*}(v)|] &= \sum_{i=1}^{\infty} s^i G(\ell(v))^{si} \prod_{j=0}^{i-1} \frac{b_j}{js+1} \\
&= s \sum_{i=1}^{\infty} G(\ell(v))^{si} \prod_{j=1}^{i-1} \frac{s \cdot b_j}{js+1} \\
&\geq s G(\ell(v))^s \sum_{i=1}^{\infty} \left(\frac{1}{(i-1)!} \cdot \left(\frac{s G(\ell(v))^s}{s+1} \right)^{i-1} \right) \\
&= s G(\ell(v))^s \cdot e^{\frac{s}{s+1} G(\ell(v))^s}.
\end{aligned}$$

The final equality again comes from the Taylor series e^x , this time evaluated at $x = \frac{s}{s+1} \cdot G(\ell(v))^s$. \square

Note that Equation A.1 does not require the assumption that n is large. Now we can use Equation A.1 and Theorem 5.1 to prove Lemma 5.3.

Lemma 5.3. *If $\text{pdf}_n(x) = \text{pdf}_e(x, y) = U([0, 1]) \forall x \in A$, then $\mathbb{E}[\{v \mid v = \text{LS}^*(v)\}] = \frac{n}{s+1}$ and*

$$\mathbb{E}[\{v \mid \ell(\text{LS}^*(v)) - \ell(v^*) \leq \epsilon\}] = n \sum_{i=0}^{\infty} \left(\frac{s^i (1 - (1 - \epsilon)^{(i+1)s+1})}{(i+1)s+1} \cdot \prod_{j=0}^{i-1} \frac{b_j}{js+1} \right).$$

Proof. The probability density function of $U([0, 1])$ is equal to 1 on $[0, 1]$ and 0 otherwise. Let $\ell(v) = x$. Then $\int_x^{\infty} \text{pdf}_e(x, y) dy = \int_x^1 dy = (1 - x)$. Using Theorem 5.1, we have

$$\mathbb{E}[\{v \mid v = \text{LS}^*(v)\}] = n \int_{\ell(v^*)}^{\infty} 1 \cdot (1 - x)^s dx = \frac{n}{s+1}.$$

Now we plug in Equation A.1 to the second part of Theorem 5.1.

$$\begin{aligned}
\mathbb{E}[\{v \mid \ell(\text{LS}^*(v)) - \ell(v^*) \leq \epsilon\}] &= n \int_{\ell(v^*)}^{\ell(v^*)+\epsilon} 1 \cdot (1 - x)^s \sum_{k=0}^{\infty} \mathbb{E}[|\text{LS}^{-k}(x)|] dx \\
&= n \int_{\ell(v^*)}^{\ell(v^*)+\epsilon} (1 - x)^s \sum_{k=0}^{\infty} \left(s^k (1 - x)^{sk} \cdot \prod_{i=0}^{k-1} \frac{b_i}{is+1} \right) dx \\
&= n \sum_{k=0}^{\infty} \left(\frac{s^k (1 - (1 - \epsilon)^{(k+1)s+1})}{(k+1)s+1} \cdot \prod_{i=0}^{k-1} \frac{b_i}{is+1} \right).
\end{aligned}$$

\square

B Details from Section 6

In this section, we give details and supplementary results for Section 6. We start by giving full details for all search spaces used in our experiments.

NASBench-101 [39]. The NASBench-101 benchmark dataset consists of over 423,000 unique neural architectures from a cell-based search space, and each architecture comes with precomputed validation, and test accuracies for 108 epochs on CIFAR-10.

The search space consists of a cell with 7 nodes. The first node is the input, and the last node is the output. The remaining five nodes can be either 1×1 convolution, 3×3 convolution, or 3×3 max pooling. The cell can take on any DAG structure from the input to the output with at most 9 edges. The hyper-architecture consists of nine cells stacked sequentially, with each set of three cells separated by downsampling layers. The first layer before the first cell is a convolutional layer, and the hyper-architecture ends with a global average pooling layer and a fully connected layer.

The neighbors of a cell consist of the set of all cells that differ by one operation or edge. Since each cell can have between 1 and 9 edges, the number of neighbors of a cell can range from 1 to 29.

NASBench-201 [8]. The NASBench-201 dataset consists of over 15,000 unique neural architectures, with precomputed training, validation, and test accuracies for 200 epochs on CIFAR-10, CIFAR-100, and ImageNet-16-120.

The search space consists of a cell which is a complete directed acyclic graph over 4 nodes. Therefore, there are $\binom{4}{2} = 6$ edges. Each *edge* takes an operation, and there are five possible operations: 1×1 convolution, 3×3 convolution, 3×3 avg. pooling, skip connect, or none. The hyper-architecture consists of 15 cells stacked sequentially, with each set of five cells separated by residual blocks. The first layer before the first cell is a convolution layer, and the hyper-architecture ends with a global average pooling layer and a fully connected layer.

Since every cell has exactly 6 edges, the total number of possible cells is $5^6 = 15625$. We say that two cells are neighbors if they differ by exactly one operation. Then the diameter of the neighborhood graph is 6, because any cell can reach any other cell by swapping out all 6 of its operations. Each cell has exactly 24 neighbors, because there are 6 edges, and each edge has 4 other choices for an operation. The neighborhood graph is $(K_5)^6$, that is, the Cartesian product of six cliques of size five.

DARTS search space [21]. The DARTS search space is a popular search space for large-scale NAS experiments. It is a convolutional cell-based search space used for CIFAR-10. The search space consists of two cells, a convolutional cell and a reduction cell, each with six nodes. The hyper-architecture stacks k convolutional cells together with one reduction cell. For each cell, the first two nodes are the outputs from the previous two cells in the hyper-architecture. The next four nodes contain two edges as input, creating a DAG. Each edge can take on one of seven operations.

B.1 Details and additional local search experiments

In this section, we give details and additional experiments for local search on the datasets described above.

For every benchmark NAS algorithm, we used the code directly from its corresponding open-source repository. For regularized evolution, we changed the population size from 50 to 30 to account for fewer queries. For NASBOT, which was designed for macro (non cell-based) NAS, we computed the distance between two cells by taking the earth-mover’s distance between the set of row sums, column sums, and node operations, similar to [36]. We did not change any hyperparameters for the other baseline algorithms. For vanilla Bayesian optimization, we used the ProBO implementation [24]. Our experimental setup is the same as prior work (e.g., [39]). At each timestep t , we report the test error of the architecture with the best validation error found so far, and we run 200 trials of each algorithm and average the result.

Table 2: Statistics of local search for NASBench-201 datasets.

Dataset	query_until_lower	Avg. path length	# local min.	% reached global min.
CIFAR-10	No	5.36	21	47.4
CIFAR-100	No	5.59	29	58.5
ImageNet-16-120	No	4.67	47	10.9
Random	No	2.56	616	0.717
CIFAR-10	Yes	9.59	21	59.8
CIFAR-100	Yes	7.31	1	100.0
ImageNet-16-120	Yes	13.33	1	100.0

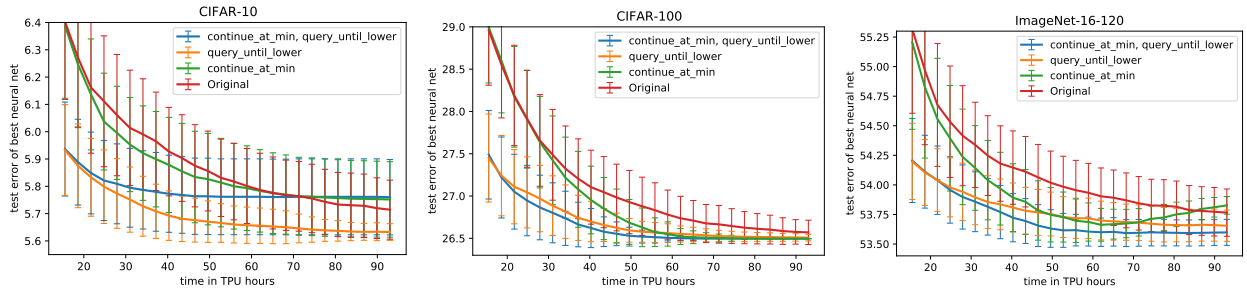


Figure B.1: Results for local search variants on CIFAR-10 (left), CIFAR-100 (middle), and ImageNet-16-120 (right) on NASBench-201.

First, we compute local search statistics for each of the datasets in NASBench-201. The experimental setup is the same as in Section 6. We also construct a randomized dataset by replacing the validation error for each architecture in NASBench-201 with a number drawn from $U([0, 1])$. For the three image datasets, we ran standard local search as well as the `query_until_lower` variant. For each experiment, we started local search from *all* 15625 initial seeds for local search, and averaged the results. See Table 2.

Now we evaluate all four variants of local search on all three NASBench-201 datasets. We use the same experimental setup as described in Section 6. See Figure B.1. See Section 5 for an explanation of the `query_until_lower` and `continue_at_min` variants to local search.

Now we evaluate the performance of local search as a function of the number of initial random architectures drawn at the beginning. We run local search with the number of initial random architectures set to 1, and 10 to 100 in increments of 10. For each number of initial random architectures, we ran 2000 trials and averaged the results. See Figure B.2.

B.2 Details from simulation experiments

In this section, we give more details for our simulation experiment described in Section 6.

For convenience, we restate Equation 6.1, the function used to approximate the datasets in NASBench-201.

$$\text{pdf}(u) = \begin{cases} \frac{1}{\sigma\sqrt{2\pi}} \cdot e^{-\frac{1}{2}\left(\frac{u-v}{\sigma}\right)^2} \cdot \left(\int_0^1 \frac{1}{\sigma\sqrt{2\pi}} \cdot e^{-\frac{1}{2}\left(\frac{w-v}{\sigma}\right)^2} dw\right)^{-1} & \text{if } u \in [0, 1], \\ 0 & \text{otherwise.} \end{cases}$$

This is a normal distribution with mean $u - v$ and standard deviation of σ , truncated so that it is a valid PDF

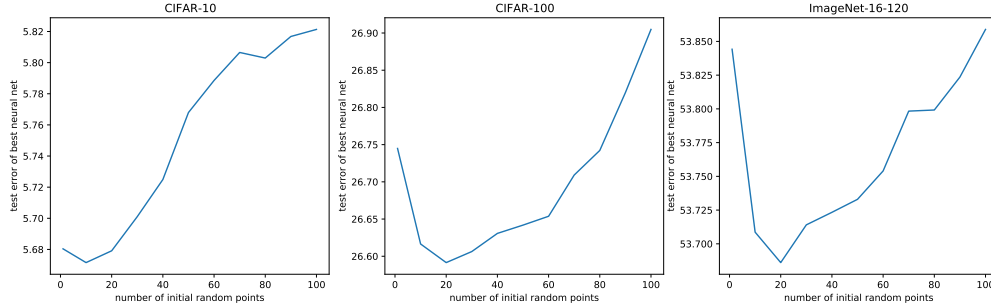


Figure B.2: Results for local search performance vs. number of initial randomly drawn architectures on NASBench-201 for CIFAR-10 (left), CIFAR-100 (middle), and ImageNet-16-120 (right).

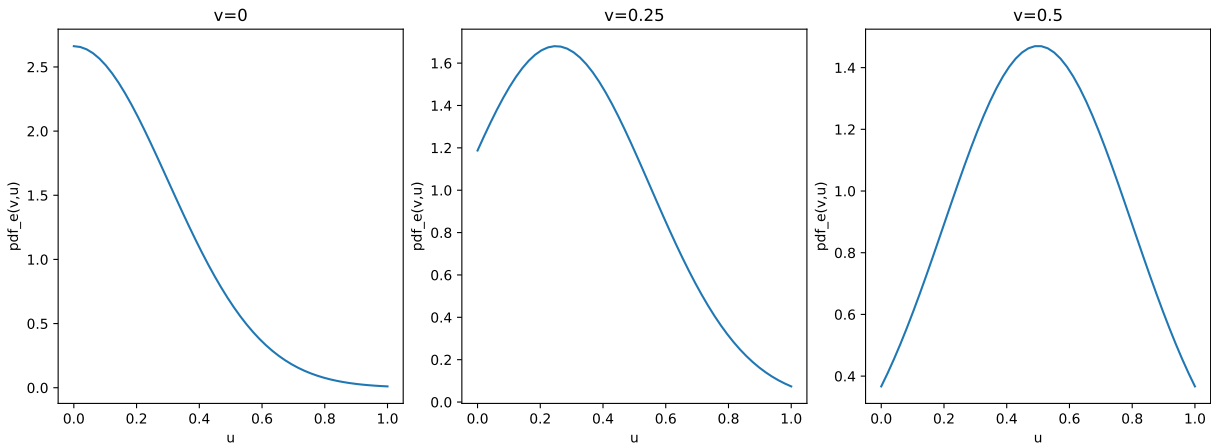


Figure B.3: Normal PDF from Equation 6.1 plotted with three values of v .

in $[0, 1]$. For a visualization, see Figure B.3. In order to choose an appropriate probability density function for modelling the datasets in NASBench-201, we approximate the σ values for both the local and global PDFs.

To model the global PDF for each dataset, we plot a histogram of the validation losses and match them to the closest-fitting values of σ and v . See Figure 6.2 in Section 6. The best values are $\sigma = 0.18$, 0.1 , and 0.22 for CIFAR-10, CIFAR-100, and ImageNet16-120, respectively.

Now we plot the random-walk autocorrelation (RWA) described in Section 6. Recall that RWA is defined as the autocorrelation of the accuracies of points visited during a walk of random single changes through the search space [34, 32], and was used to measure locality in NASBench-101 in prior work [39]. We compute the RWA for all three datasets in NASBench-201, by performing a random walk of length 100,000. See Figure B.4. We see that all three datasets in NASBench-201, as evidenced because there is a high correlation at distances close to 0. As the diameter of NASBench-201 is 6, the correlation approaches zero at distances beyond about 3.5. In order to model the local pdfs of each dataset, we also compute the RWA for Equation 6.1, and match each dataset with the closest value of σ . We see that a value of $\sigma = 0.35$ is the closest match for all three datasets.

Now for each of the three NASBench-201 datasets, we have estimates for the pdf_e and pdf_n distributions. We plug each $(\text{pdf}_e, \text{pdf}_n)$ pair into Theorem 5.1, which gives a plot of ϵ vs. percent of architectures that

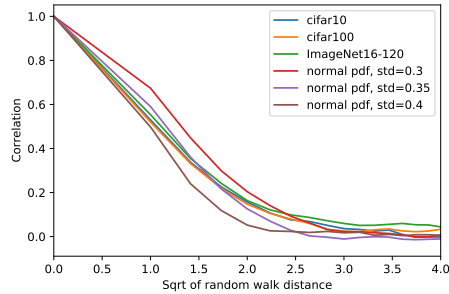


Figure B.4: RWA vs. distance for three datasets in NASBench-201, as well as three values of σ in Equation 6.1. Since a random walk reaches a mean distance of \sqrt{N} after N steps, we plot the x -axis as the square root as the autocorrelation shift, similar to prior work [39].

converge to within ϵ of the global optimum after running local search. We compare these to the true plot in Figure 6.3. For the random simulation, we are modeling the case where $\text{pdf}_e = \text{pdf}_n = U([0, 1])$, so we can use Lemma 5.3 directly.

B.3 Best practices for NAS research

The area of NAS research has had issues with reproducibility and fairness in empirical comparisons [18, 39], and there is now a checklist for best practices [19]. In order to promote best practices, we discuss each point on the list, and encourage all NAS research papers to do the same.

- **Releasing code.** Our code is publicly available at https://github.com/realityengines/local_search. The training pipelines and search spaces are from popular existing NAS work: NASBench-101, NASBench-201, and DARTS. One thing that is missing is the set of random seeds we used for the DARTS experiments.
- **Comparing NAS methods.** We made fair comparisons due to our use of NASBench-101 and NASBench-201. For baseline comparisons, we used open-source code, a few times adjusting hyperparameters to be more appropriate for the search space. We ran ablation studies, compared to random search, and compared performance over time. We performed 200 trials on tabular benchmarks.
- **Reporting important details.** Local search only has two boolean hyperparameters, so we did not need to tune hyperparameters. We reported the times for the full NAS method and all details for our experimental setup.